

Review

A Review of Lithium-Ion Battery Thermal Management System Strategies and the Evaluate Criteria

Shuting Yang^{1,2,3}, Chen Ling^{1,2,3}, Yuqian Fan⁴, Yange Yang^{1,2,3}, Xiaojun Tan^{4,*}, Hongyu Dong^{1,2,3,*}

¹ School of Chemistry and Chemical Engineering, Henan Normal University, Xinxiang, Henan Province, 453007, China;

² National & Local Engineering Laboratory for Motive Power and Key Materials, Xinxiang, Henan Province, 453007, China;

³ Collaborative Innovation Center of Henan Province for Motive Power and Key Materials, Xinxiang, Henan Province, 453007, China;

⁴ School of Intelligent Systems Engineering, Sun Yat-sen University, Guangzhou, Guangdong Province, 510006, China;

*E-mail: tanxj@mail.sysu.cn (X. Tan); donghy373@163.com (Y. Dong)

Received: 7 December 2018 / Accepted: 26 March 2019 / Published: 10 June 2019

Lithium-ion batteries have become widely used in energy storage systems. Since adverse operating temperatures can impact battery performance, degradation, and safety, achieving a battery thermal management system that can provide a suitable ambient temperature environment for working batteries is important. This paper provides a review based on previous studies, summarizes the electrical and thermal characteristics of batteries and how they are affected by the operating temperature, analyzes the relative merits and specific purposes of different cooling or heating methods, and provides many optimization methods. Moreover, because low power consumption, a high temperature regulation capacity, and excellent temperature uniformity are desired for every battery thermal management system, we also present control strategies that can contribute to thermal management. It is indispensable to establish criteria to evaluate battery thermal management systems. We subsequently summarize the characteristic parameters for the analysis of various battery thermal management system designs. Finally, we provide an outlook for the development of lithium-ion battery thermal management systems.

Keywords: Lithium-ion battery; thermal characteristic; thermal management system; control strategies; evaluate criteria.

1. INTRODUCTION

With growing concerns over fossil fuel depletion and the increasing price of crude oil, electric vehicles have gained more interest as a mode of transportation [1]. Various electric vehicles have been

developed in recent years, including pure electric vehicles (EVs), hybrid electric vehicles (HEVs), and plug-in hybrid electric vehicles (PHEVs).

One keen focus area in the ongoing development of electric vehicles is their energy storage systems. At present, lithium-ion batteries are used extensively for automobiles. They include Li-Co lithium-ion (LCO), Li-Fe lithium-ion (LFP), Li-Mn lithium-ion (LMO), and Li-NiCoMn lithium-ion (NCM) batteries. When batteries are charging/discharging, various complicated reactions occur. In addition, the thermal behaviors of the batteries are coupled to these reactions [2]. Electrochemical reactions affect the heat generation rate, and higher temperatures further increase the speed of the electrochemical reactions [3]. To optimize their performances, it is necessary to understand the characteristics of the specific battery.

As previous research has shown, battery performance is highly dependent on the working ambient temperature. Batteries have a higher request in the working ambient temperature. For example, the battery state of health (SOH) is influenced by temperature significantly. Battery life may be reduced by 2/3 in hot climates during aggressive driving and without cooling [4]. If a lithium-ion battery operates at a lower ambient temperature long-term, high specific surface area lithium dendrites form on the anode of the battery, resulting in a rapid decrease in the battery's SOH [5]. With a battery temperature exceeding the stable point, severe exothermic reactions occur uncontrollably [6]. In addition, if a battery approaches thermal runaway, only 12% of the total heat released in the battery is enough to trigger thermal runaway in adjacent batteries [7]. This is the biggest risk during the use of lithium-ion batteries.

As discussed above, batteries' working temperatures play significant roles in energy storage systems. Thermal-related research on batteries has been performed previously. One of the aspects studied is improving battery heat stability performance and lowering the risk of thermal runaway, which is influenced by the characteristics of the electrode, such as the materials [8-10], electrolyte [11], and separator [12]. Characteristics of battery thermal runaway processes differ with the variation of the battery material [13]. Another approach is to add thermal control components to provide suitable working conditions for batteries, referred to as a battery thermal management system (BTMS).

A BTMS is a necessary component of lithium-ion battery systems, especially at high ambient temperatures [14]. There are two main functions of BTMSs: 1) to keep batteries working under suitable conditions and improve the electrical performance and battery life and 2) to prevent thermal runaway from occurring and improve safety. Most battery thermal management methods, such as air cooling, liquid cooling, and phase change material (PCM) cooling, have been reviewed previously [15]. Furthermore, different cooling/heating methods and optimization strategies have been discussed, and the relevant cooling/heating performances were analyzed. In general, there are two demands for BTMSs: 1) the maximum/minimum temperature of batteries must remain within the operating temperature range limit and 2) the non-uniform temperature distribution must remain within the range of the reference limit.

To prevent thermal runaway from occurring and maintain a favorable working performance, serial measurements should be made to cool/heat batteries appropriately, and designing the thermal path to expel the combustion of electrolyte away from adjacent cells [16]. There are three main types of heat transmission patterns, heat conduction, heat convection, and radiation, which determine the

cooling/heating performance. For example, natural convection and forced convection are two different heat convection modes. In the former mode, the battery system can operate well with a low heat generation rate. However, failure occurs at a high heat generation rate because the heat of the battery system cannot be removed quickly enough. In the latter mode, the maximum temperature of the battery system can be reduced, but it may increase the temperature deviation [17].

A non-uniform temperature distribution is related to the battery/pack geometric features, charge/discharge rate, ambient temperature [18], and cooling rate [19]. For a single battery, the battery's surface area to volume ratio has a significant effect on the non-uniform temperature distribution. Different locations of battery current collecting tabs and the ratio of the battery's length and width distinctly affect the uneven distribution of the current density [20]. An appropriate battery geometry design can produce a uniform temperature through parameters such as the length to width ratio [19, 21], location of current collecting tabs [22], and the ratio of volume and surface area [23-24]. In a pack, the position of the battery may cause slight differences in the cooling effect and operating current, which may lead to a non-uniform temperature distribution. Less temperature uniformity results in the rapid decay of the cycle life of the battery pack. Even worse, the non-uniform temperature distribution may aggravate the unbalanced discharging phenomenon and decreases the available energy for the battery packs [25].

For a BTMS, dissipation of the internal heat of the pack by improved heat transfer is insufficient. A combination of an appropriate cooling strategy, the pack's structure, and the rate of charge/discharge is required to design a suitable BTMS for special packs [26]. In the future, a multi-objective optimization algorithm [27] should be employed. In addition, before designing a BTMS for a specific battery pack, the following questions should be answered [28]: (1) How much heat must be removed from the pack? (2) What are the allowable temperature maximum and difference? (3) Which kind of heat transfer pattern is needed? (4) Is active cooling required? (5) What is the extra cost of the BTMS?

Numerous methods have been proposed in previous studies to improve the cooling performance. For air or liquid cooling, for example, increasing the coolant velocity or the size of cooling structure may benefit the average temperature and temperature uniformity. However, the cost of such optimization increases the pack volume, resulting in a larger power consumption of the BTMS. There have been no uniform standards created to judge cooling/heating designs, and few researchers have demonstrated the features of different cooling/heating strategies and determined the conditions for which they are suitable.

Previous reviews [29-30] have analyzed BTMSs in detail. This study aims to supplement and look to future developments based on the latest research. Specifically, an overview of the electrical and thermal characteristics of lithium-ion batteries is provided, the heat generation feature of batteries are summarized, the cooling performances of different thermal management methods are analyzed, different optimization methods are summarized and compared, an of overview of the control strategies for BTMSs is presented, the importance of the control strategies for BTMSs are discussed, and the use of the BTMS properties as evaluation criteria to judge whether the design BTMS is appropriate is presented.

The rest of this article is structured as follows: The electrical and thermal characteristics of batteries are introduced in Section 2. Strategies for battery cooling/heating are analyzed in Section 3. Control strategies and evaluation criteria for BTMSs are provided in Section 4. Finally, the conclusions and outlook are presented in Section 5.

2. BATTERY CHARACTERISTICS

Electrode materials and dimensions of batteries determine their properties. Before design an energy storage system, it should be noted that the electrical characteristics of the battery, such as current, voltage, and capacity, and thermal characteristics, such as battery performance when working at different ambient temperature. This section focuses on the electrical and thermal characteristics of lithium-ion batteries. The theoretical model and simulation for thermal characteristics of batteries or packs are summarized.

2.1. Electrical characteristics

Battery electrical performance is related to charge/discharge rate, ambient temperature [31] and SOH [32], which is shown clearly in available capacity [33], working voltage platform and internal resistance [34]. Firstly, with an increasing of battery discharge rate, operating voltage platform of batteries becomes lower and shorter, lesser energy released before it meets the cut-off voltage (Figure 1(a)), and the equivalent internal resistance becomes smaller [35-38]. Secondly, reducing the ambient temperature can lower the working voltage platform of batteries as well [39] (Figure 1(b)). The essential reason is that the electrochemical parameters of battery are changing with its states and the operating condition [40].

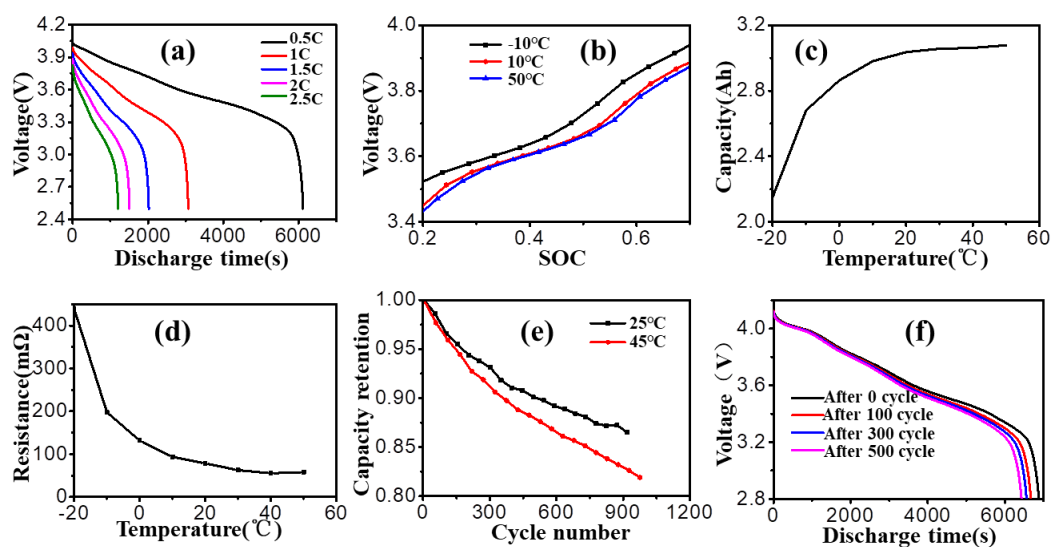


Figure 1. (a) Battery voltage profiles during discharging at different rate; (b) Open circuit voltage (OCV) at different temperature; (c-d) Lithium-ion batteries capacity and resistance at different temperature; (e) Batteries capacity retention of high temperature battery (HTB) and room temperature battery (RTB); (f) Terminal voltage of lithium-ion battery at constant current (CC) discharge during different SOH.

If the operating temperature is adjacent to 0°C, the available capacity will decrease rapidly, and the internal resistance will increase spectacularly (Figure 1(c-d)). Finally, the decreasing rate of battery capacity will be magnified obviously at the higher operating temperature (Figure 1(e)), as the nanostructure and crystal structure of cathode materials are destructed [41]. Regarding the aging process of lithium-ion batteries, batteries' internal resistance increases gradually, and the terminal voltage becomes lower at the same working current [42] (Figure 1(f)).

There are four methods to acquire battery internal resistance [43]: voltage-current(V-I) characteristics, resistance by over-potential, rapidly intermittent charge/discharge and AC impedance spectroscopy. Equivalent internal resistance of battery can be measured by the Galvanostatic Intermittent Titration Technique (GITT) [44]. The battery is put into a climatic chamber to control its ambient temperature, and charge or discharge for short pulse separated by rest periods [45]. The voltage difference of battery at beginning and ending of the rest period, which can be seen as specific voltage consumed by internal resistance include ohmic resistance and polarization resistance. The method based on over-potential resistance is mostly to calculate batteries heat generation performance [46].

As discussed above, batteries' equivalent internal resistance is affected by SOC, SOH and ambient temperature. In addition, electrochemical impedance spectroscopy (EIS) [33, 47-48] is also affected by these factors. All of these characteristics should be considered to estimate battery state or acquisition battery heat generation performance.

2.2 Thermal characteristics

Temperature has a great influence on a battery. Generally, a higher temperature can speed up the chemical reaction. However, according to the thermal characteristics of specific batteries, charging/discharging for batteries in more comfortable ambient contributes to the process of electrochemical reaction; any excessively high or low temperature may encourage undesired side reaction or structure damage.

2.2.1. Battery heat generation

Lithium-ion batteries heat generation rate is strongly related to the working environment and their own state [49]. In addition, the higher charging/discharging rate, the fiercer the battery temperature increase [50-51]. The published literatures have presented two approaches to obtain battery heat generation rate: theoretical calculation and experimental measurement.

Bernardi [52] first purposed a computational method to predict battery temperature and heat generation rate, according to energy-balance equation and Gibbs function, it presented that batteries temperature changed with electrochemical reactions, phase changes, mixing effects and joule heating. And the battery heat generation equation can be simplified as irreversible heat (enthalpy changes) and reversible heat (entropic-heat) [53-54] (Eq. (1-3)).

$$Q_{tot} = Q_{irr} + Q_{rev}, \quad (1)$$

$$Q_{irr} = R_{int}I^2, \quad (2)$$

$$Q_{rev} = -IT \frac{\partial E_{eq}}{\partial T}, \quad (3)$$

where Q_{tot} is battery total heat generation rate; Q_{irr} and Q_{rev} are the heat generation rate of irreversible and reversible, respectively; R_{int} is battery equivalent internal resistance; I is working current; T is battery temperature; and E_{eq} is equilibrium electromotive force at specific SOC.

Enthalpy changes were always calculated by the internal resistance based on over-potential [46]. Battery entropic-heat was associated with the materials of cathodes and anodes [55-56], and usually acquired by experiment, such as the references [46, 57] measured the data of entropic-heat by means of plus current. And this method can save a lot of time at the cost of enlarging-errors slightly.

Battery thermal behavior is still complex, LCO battery, for example, equivalent internal resistance will increase with the decrease of ambient temperature or the increase of discharging duration time, which means that the irreversible heat of battery is changing with ambient temperature and the discharge process. Furthermore, the entropy changes of battery exhibit great difference at different SOC states [58] (Figure 2). Moreover, the proportion of entropic-heat could not be ignored at low charge/discharge rate and which may be diminished with the increase of charge/discharge rate [19].

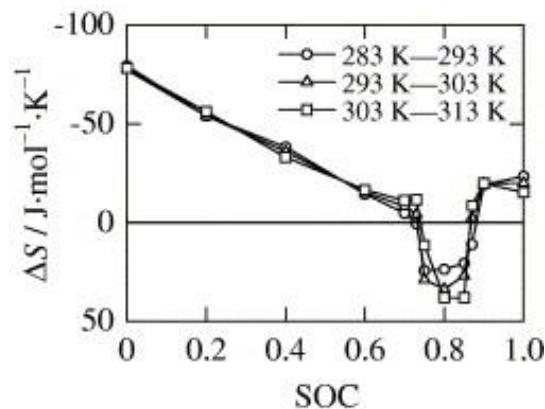


Figure 2. Experiment results of LiCoO₂ batteries entropy change (“Reprinted from Energy Conversion and Management, 48, Y. Inui, Y. Kobayashi, Y. Watanabe, Y. Watase, Y. Kitamura, Simulation of temperature distribution in cylindrical and prismatic lithium ion secondary batteries, 2103-2109, Copyright(2007), with permission from Elsevier.”).

For experimental method, E. Schuster [59] acquired batteries heat generation rate by three different methods (adiabatic condition experiment, isoperibolic condition experiment and theoretical calculation with irreversible and reversible heats), and the results showed a generally good agreement. However, significantly difference of heat generation rate may occurred during rapid charging/discharging between adiabatic and isoperibolic condition, it is due to battery heat generation rate is related to the temperature changes [60], battery temperature become higher and the heat generation rate become lower as well [61].

What’s more, before designing an efficient BTMS, it is necessary to acquire two major parameters of batteries: heat capacity and thermal conductivity. Several factors affect this two

parameters: For batteries, the thermal conductivity increases with the electrode and separator infiltrated by electrolyte and then the heat conductivity coefficient are increasing [62]; In-plane has a larger thermal conductivity than through-plane because of the high value of current collector [63] and thermal transport is limited by the interface thermal resistance [64]. In addition, the thickness of batteries electrode also affect batteries heat capacity and thermal conductivity [65-66]. In ambient temperature, batteries heat capacity is increased linearity with temperature [65], while the thermal conductivity decrease at over-lower [66] or over-higher ambient temperature [67], and after several times cycle at high ambient temperature, batteries thermal conductivity of decreases as well, this is due to gas generated by electrolytes deposition and side reactions in the battery [63].

Table 1. Summary of lithium-ion battery main thermal physical parameters.

Battery	Shape	Capacity (Ah)	Density (kg*m ⁻³)	Heat capacity (J*kg ⁻¹ *K ⁻¹)	Thermal conductivity (W*m ⁻¹ *K ⁻¹)
LCO [68]	Prismatic	20	2663	1068.51	31.59
LFP [69]	Cylindrical	1.5	2663	900	Radial: 3; Axial: 30
LFP [70]	Cylindrical	-	2450	1108.4	Radial: 3.917
LFP [71]	Cylindrical	8	2461.5	1605	Radial: 0.2; Axial: 37.6
LFP [72]	Prismatic	40	2300	1280	2.73
LFP [73]	Prismatic	100	1676	1100	in-plane: 2.7; through-plane: 0.9
LFP [74]	Prismatic	20	2285	1605	32
LFP [75]	Pouch	10	2054.39	1200	in-plane: 18.4; through-plane: 0.34
NCM [57]	Cylindrical	2.3	2047.3	890	Radial: 0.4
NCM [76]	Cylindrical	2.6	2700	900	7.14
NCM [77]	Cylindrical	2.5/3.2/10	1760	1108	3.91
NCM [78]	Pouch	15	2400	1015	30
LMO [79]	Cylindrical	3.6	2007.7	837.4	32.2
Li-ion* [80]	Prismatic	15	2335	745	in-plane: 27; through-plane: 0.8
LTO^ [44]	Prismatic	20	1957.1	901.961	0.5

*Lithium-ion battery, and more specific information were unknown.

^ Lithium titanate battery.

Considering composition of the battery, previous studies [62, 67, 81] calculated battery heat capacity and thermal conductivity according to the parameters of different materials and its ratio composed for batteries, respectively. In the meantime, many researchers identify the battery heat properties by experiments as well. Damay [45] wrapped prismatic LFP battery with insulating materials for adiabatic. It is being heated by $\pm 1C$ rectangular current with a period of 20 seconds, and then the heat capacity is determined by Eq. (4).

$$C_p = \frac{Q_{tot}}{dT/dt}, \quad (4)$$

where C_p is battery heat capacity; dT/dt is the variation rate of battery internal temperature with time. According the first law of thermodynamics, Christophe [82] calculated cylindrical LFP battery C_p by Eq. (5). However, there is an obvious question that it is hard to acquire the heat resistance accurately. The calculate result is significantly different with the increase of current pulse magnitude.

$$\frac{dT_{surf}}{dt} = \frac{T_{amb} - T_{surf}}{C_p(R_{int} - R_{out})} + \frac{Q_{tot}R_{out}}{C_p(R_{int} - R_{out})}, \quad (5)$$

where T_{surf} is battery surface temperature; T_{amb} is test ambient temperature; R_{int} is thermal conductivity resistance from the core of battery to surface; R_{out} is heat convection resistance from the battery surface to ambient. Parsons [83] discussed the use of heat preservation equipment to measure C_p , this method can ignore the non-uniform distribution of temperature of inner batteries. In addition, considering the effects of the lag of thermal response, compensation by batteries time constant may acquire more precisely C_p [43, 84]. Accelerating Rate Calorimeter (ARC) has been successfully applied in battery research [85-87], which can provide an almost adiabatic conditions for tests. Schuster [59] embedded a small heat mat into the middle of two pouch batteries to ensure that all the heat generation of the mat was conduction to the two batteries, and set batteries into ARC. Keeping the increasing rate of batteries temperature is constant as 0.02K/min through adjusting the heat generation rate of mat. And finally acquired the heat capacity of $\text{LiC}_6/\text{Li}(\text{Ni}_{1/3}, \text{Mn}_{1/3}, \text{Co}_{1/3})\text{O}_2$ pouch batteries and fitted by the heat balance equation (Eq. (6)).

$$C_p = 0.96 + 0.005T - 1.86 \cdot 10^{-5}T^2 [\text{J/g} \cdot \text{K}], \quad (6)$$

where the limitation of T is in 25~60°C. Further studies about lithium-ion battery heat capacity and thermal conductivity were summarized in Table 1.

2.2.2. Thermal runaway

Battery safety attracts the close attention of users. Batteries working at too high temperature ambient may lead to volume swelling, and non-uniform temperature distribution has an effect on the batteries thermal stress and strain and result in different swelling shapes. All of them are very important for battery safety and lifetime [88]. What is worse, short-circuit [89] and overheating [90] most likely cause thermal runaway. When thermal runaway occurs, serious exothermic reaction will come one after another [24, 91]: solid electrolyte interphase (SEI) layer decomposition, negative electrode-electrolyte reaction, electrolyte decomposition and positive electrode-electrolyte reaction [92]. LFP, for example, SEI layer decomposed at 100°C, separator melting and shrinking at 143°C, and the thermal runaway takes place when temperature over than 150°C [93]. In addition, if causing fire and explosion, oxygen generated by electrolyte reaction may aggravate the terrible state [92]. In addition, with the rapid release of a large amount of energy [94], a large quantity of toxic gas will threaten personal safety [95].

Generally, single battery thermal runaway may happen via three factors [96]:

- 1) Internal thermal resistance fault, such as swelling gas existed in the core of battery can increasing thermal resistance dramatically.
- 2) Heat generation fault, such as a short-circuit leading to uncontrollable heat generation.

3) Outer convective cooling fault, such as when battery heat could not be removed to outer in an adiabatic condition.

Battery safety is determined by its materials. Experiments by Jiang [85] indicate that LFP exhibits higher thermal stability than NCM and LCO. Furthermore, LiPF_6 , main components of the electrolyte, is suitable for LFP, while LiBOB is suitable for NCM and LCO. Battery thermal characteristics are always also contingent on its state. Wang [97] tested LFP and NCM batteries at different SOC. The research indicates that thermal runaway reaction is sensitive with SOC, the higher SOC batteries intensify risk of thermal runaway [94, 98]. For fresh batteries, with SOC increasing, the thermal runaway occurring temperature may decrease, and more gas will be generated; For aged batteries, there are no significant changes of thermal runaway occurred temperature, and fewer joule heat released by the batteries [5].

As for safety, solid state rechargeable batteries have an advantage over liquid batteries. There are still many impediments to commercialization [26]. In addition, there are other technologies to prevent thermal runaway such as adding inhibitor to battery materials [6, 99], which can increase the temperature of thermal runaway occurred point. In the state-of-the-art, there is still no effective strategy to solving batteries aging at high temperature. Thus, the best way to prevent thermal runaway in batteries is to design an appropriate BTMS for packs. For the safety of a lithium-ion battery pack, the purpose of designing a BTMS is to improve thermal abuse tolerance and obstruct the spread of thermal runaway [100].

2.3 Theory model and simulation

Theory model and simulation is quite important for batteries or packs during the process of designing a BTMS. The aim is to simulate batteries working states, optimize the thermal management project [101], improve life and performance of the pack, and estimate the safety of the designed system [102].

2.3.1. Heat generation model

For the purpose of estimating SOC and electrical parameters accurately, various equivalent circuit models are widely used [103], such as the RC model [45], the Thevenin model, the PNGV model and the DP model [104]. In addition, considering the influence of temperature, electrical-thermal coupled model [14, 105-106] and electrochemical-thermal coupled model [107] are developed. Furthermore, considering the influence of SOH, non-uniform state in different position for larger size batteries and other mechanical structure of packs, multi-dimensional model is employed for batteries or packs [78, 108]. Previous reviews have presented more exhaustive introductions for these models [29-30]. In this article, we emphatically discuss two key issues about the heat generation model: temperature distribution in a battery model and battery temperature global estimation.

Two main reasons cause temperature gradient in a single battery. One is different current density leading to heat generation non-uniformity. Although heat generation rate during charging is

less than discharging, the battery is most prone to catastrophic failure during charging [109]. It is due to the temperature rising rapidly and significantly in local position especially in the battery positive current tab [102] (Figure 3(a)). Lin [110] performed an 100Ah lithium-ion battery short-circuit experiment and revealed that only battery tab temperature increased rapidly in a very short time. Another temperature gradient exists between the surface and the core of battery because of different thermal response time [111] (Figure 3(b)).

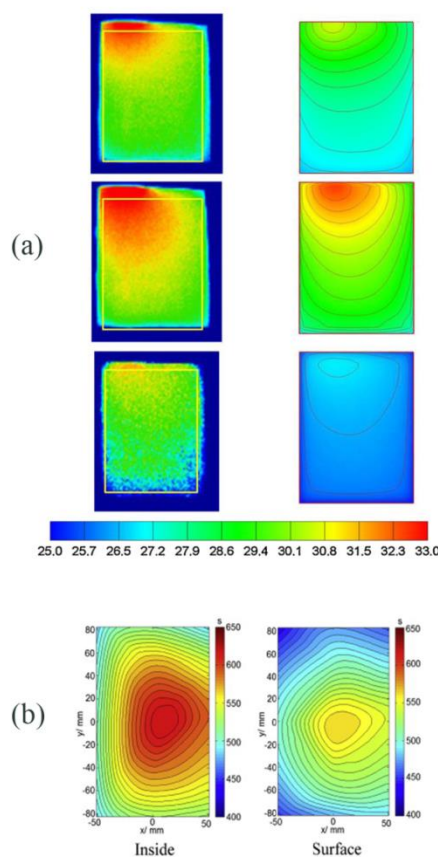


Figure 3. (a) Temperature distributions of soft packing batteries based on experimental Infrared Ray image and modeling at charge times of 8min, 16 min and 36 min during constant current and constant voltage charging with CC charge at 3C (“Reprinted from Journal of Power Sources, 196, U.S. Kim, J. Yi, C.B. Shin, T. Han, S. Park, Modelling the thermal behaviour of a lithium-ion battery during charge, 5115-5121, Copyright(2011), with permission from Elsevier.”); (b) the distribution of lithium-ion batteries thermal response time (“Reprinted from Journal of Power Sources, 241, Z. Li, J. Zhang, B. Wu, J. Huang, Z. Nie, Y. Sun, F. An, N. Wu, Examining temporal and spatial variations of internal temperature in large-format laminated battery with embedded thermocouples, 536-553, Copyright(2013), with permission from Elsevier.”).

During the period of cooling after full discharge, comparing with the temperature of cylindrical batteries about axial direction or radial direction, it is shown that removing the thermal in the core of battery is more difficult than surface [17]. Al-Hallaj [19] has observed that there is a significant temperature gradient inside the battery at high outer cooling rate. Based on the thermal resistance

theory, Forgez [82] elicited Eq. (7) and confirmed the relationship between battery surface temperature and the core.

$$T_{in} = T_{surf} \left(1 + \frac{R_{int}}{R_{out}} \right) - T_{amb} \frac{R_{int}}{R_{out}}, \quad (7)$$

where T_{in} is temperature of the battery core; Based on the heat transfer theory, the R_{int}/R_{out} is just the Biot number, and if the Biot number is smaller than 0.1, it is suitable to ignore the temperature difference between internal and surface. And lumped-parameter thermal model can be used to simulate the thermal behavior of battery.

The core temperature of batteries affects their performance directly, and maximum temperature of batteries as a signal that whether the battery is safety or may breaking. But it is very hard to collect all the temperature data of batteries. References [112-113] introduced thermocouple into a battery to obtain internal temperature, but it is difficult to popularize in practical EV/HEV. Two approaches can be distinguished to estimate battery temperature. The one is based on the first law of thermodynamics, according to the heat generation rate, batteries surface temperature and heat dissipation rate to calculate batteries temperature [49]. The other one is depending on batteries electric characteristics in different temperature, monitoring batteries in real time and estimating batteries temperature directly. Wang [114] explored a temperature estimating method based on a neural network that could be applied to unknown boundary cooling condition. Richardson [115] demonstrated that the impedance of battery changed at varied frequencies with SOC and ambient temperature. According to a battery's SOC, impedance at 215Hz and surface temperature, a method was eventually confirmed to estimate a single battery's internal temperature distribution. Moreover, considering the battery characteristics of anisotropy, Richardson [116-117] further built a two-dimensional model by means of different arithmetic.

2.3.2. Heat dissipation model

There are three heat transfer ways: thermal conduction, thermal convection and thermal radiation, which always working for heat transfer process alone or in combination. Furthermore, battery structure is complicated; it is difficult to design a general duty heat dissipation model that can be appropriate for all species. According the characters of the battery structures to choosing the suitable cooling strategies and properly heat dissipation method is necessary for designing and optimizing BTMS.

Most lithium-ion batteries also exhibit anisotropy features. With cylindrical batteries, for example, the isothermal curves of spirally wound batteries are roughly cylindrical [24]. This phenomenon is contributed to the high thermal conduction of battery current collector in axial direction. As for pouch batteries, in-plane temperature variation is always much larger than through-plane direction although in-plane shows much larger thermal conductivity [111]. The reason is that in-plane has a longer path length of thermal conduction. Compared with large volume batteries, small volume batteries can rapidly heat/cool [24]. This is due to the small volume batteries owns higher specific surface area can used to heat transfer. In addition, it may have a similar cooling effect compared with cooling a different side surface (in-plane or through-plane for punch batteries and side

plane or end plane for cylindrical batteries) because of anisotropy as well as different cooling area and path length [3].

The thermal resistance model is suitable to analyze heat transfer problems of batteries or packs. For packs, modeling thermal resistance of the heat transfer process between batteries and cooling medium [118], heat flux can be determined by including the temperature difference (Eq. (8)), which contributes to require cooling power and temperature distribution of the cooling medium. For batteries, according to battery geometry to analyze thermal resistance distribution [45], and considering heat generation distribution, brilliant BTMS effects can be achieved through improving the cooling effect of the high-risk place.

$$\Phi = \frac{\Delta T}{R}, \quad (8)$$

Where Φ is heat flux; ΔT is thermal transfer temperature difference; R is total thermal resistance.

3. THERMAL MANAGEMENT STRATEGIES

Various cooling strategies can be used as battery thermal management, such as air cooling, liquid cooling and PCM. The cooling strategies of some new-energy automobiles BTMS were summarized in Table 2. Every thermal management strategy has its own advantages. For example, in terms of the system's cooling performance, a liquid cooling system exhibits stronger cooling performance, and phase change materials possess an outstanding ability in control temperature differences. In this section, different merits of cooling strategies are reviewed, various optimization methods of BTMS are summarized, and battery heating strategies are noted.

Table 2. Summary of new-energy automobiles battery cooling strategies

Vehicle	Class	Pack (kWh)	BTMS strategies
Nissan leaf	HEV	24	Air
Tesla model S	EV	60-85	Liquid
BMW 740Le	EV	9	Refrigeration
NIO es8	EV	70	Liquid
BYD e6	EV	82	Liquid
BMW 530Le	PHEV	13	Liquid

3.1 Air cooling

According to whether a cooling fan is needed, air cooling strategies can be categorized as natural cooling and forced cooling. The corresponding heat transfer methods are natural convection and forced convection, respectively. Radiation heat exchange always plays an important role in natural cooling and must not be ignored. Air cooling strategies can be used in special application conditions. Differing from other methods, air cooling could ensure the batteries are working at a comfortable

environment temperature when the ambient temperature nears 0°C [68]. Furthermore, the structure of an air cooling system is considerably simple and without a sealing problem. Al-Hallaj [69] compared cooling performance of force air-cold with PCM (paraffin wax-graphite), and showed that at a low ambient temperature and discharge rate, an air-cooling system has the same cooling effect with PCM but has lighter structures

Air cooling structure and the air streamline play a decisive role in pack heat dissipation performance, temperature distribution, and energy consumption of the fan [119]. Two types of classical air cooling structures, widely known [120], are the serial cooling structure and the parallel cooling structure. In particular, most topology structures based on these two structures are applied to satisfy the requirement of cooling performance. Xu [121] designed a double ‘U’ type duct for cooling the battery bottom. Liu [122] presented a parallel air cooling pack structure, in which the sub-module installed is also a parallel structure. In addition, he developed a shortcut computation for plenums plate angle and battery unit spacing at different heat generation rate and air flow velocity to meet the battery pack uniformity of flow and temperature. For pouch battery pack, there is usually no cooling channel in the adjacent batteries, thus it has to employ high thermal conductivity materials insert in the middle of two batteries, such as silica cooling plate coupled with copper mesh [123], which can improve the heat transfer effect between ambient and the core of battery pack.

Computational fluid dynamics (CFD) [77, 124-125] was always used in developing a BTMS model and simulate the cooling effect of battery, module, or battery pack. Optimized structure ensures air flow uniformity and decreases the battery pack maximum temperature, the temperature difference, and energy consumption [118].

In order to improve the cooling performance of the system, according to Newton’s law of cooling (Eq. (9)), three methods can be selected: increasing convective heat transfer, increasing heat transfer area, and increasing the temperature difference between batteries and the cooling medium.

$$\Phi = hA\Delta T, \quad (9)$$

Where h is convective heat transfer coefficient, A is heat transfer area. Convective heat transfer coefficient is a key parameter to evaluate the ability of air cooling structure, which can be gained by empirical equation of Nusselt number and Reynolds number for experiment of air cooling structure [71]. Convective heat transfer efficiency can be improved by increasing the velocity of air flow. In addition, it is efficient to decrease the battery maximum temperature by increasing air velocity. However, battery temperature uniformity will become worse [81, 126]. The reason is that the power of forced convection increasing can improve the heat transfer coefficient. The higher heat transfer performance may lead to more thermal turn into cooling air at the inlet location, whereas the temperature difference of heat transfer in the outlet location shrinks. Then it induces the cooling performance to become strengthened at inlet location and weakened at outlet location. Meanwhile, the significant cost of increasing the velocity of cooling air flow is such that the energy consumption for the fan increased exponentially [127]. In addition, Xie [128] investigated that enhancing heat transfer coefficient by vortex generators, contributes to bulk fluid mixing, boundary layer modification and flow destabilization. Increasing heat transfer performance can also be achieved by increasing the heat transfer area, such as pin fin heat sinks [126]. To improve the uniformity of heat dissipation performance in different positions of the packs, Chen [129] suggested that the space of cooling channel

around the batteries with the highest temperature should be widened while the one around the battery with the lowest temperature should be narrowed. Mohammadian [126] increased the fins area gradually from the inlet of cooling air to the outlet.

Optimizing the flow field by altering the structure of the pack is indispensable to save energy consumption and improve cooling performance [130]. Battery average temperature may present no significant difference if the pack's volume ratio of cooling channel and battery unit are equal [131]. However, the system pressure drop becomes lower when the size of the cooling channel is enlarged [80, 131-132]. In order to improve temperature uniformity of the pack, Chen [133] utilized two means which fixed inlet flow rate and fixed the fan's power consumption to optimize a parallel air-cooling structure through altering the widths of divergences plenum and convergences plenum. Moreover, optimizing the airflow inlet and outlet position should be considered when designing an air cooling structure. Based on the overall consideration of battery maximum temperature, the space utilization and the energy efficiency, Lu [134] purposed designing the airflow inlet and outlet that are located on the top of battery pack can achieve the best cooling performance. In addition, the internal airflow might be affected by the external air flow field when the automobile is driving, thus the appropriate position of airflow inlet and outlet should consider to avoid the obstacles of external air flow [135].

According to Eq. (9), although improving the temperature difference for heat transfer can ameliorate heat transfer capacity, battery temperature deviation from air inlet to outlet is enlarged [126]. Lowering the temperature of an inlet cooling medium does not represent a constant effective method. According to the field synergy principle, He [130] discussed that increasing the flow rate and lowering the temperature difference between inlet medium and batteries can promote the temperature homogeneity of batteries. Mahamud [79] proposed a reciprocating air flow system devoted to battery thermal equilibrium. The results indicated that increasing reciprocate frequency can reduce temperature difference and the maximum battery temperature. He [136] also indicated that, under the same goal of maximum battery temperature control, reciprocating cooling flow is superior to other air cooling strategies due to its lower air flow rate and temperature difference.

Although the air cooling strategy can achieved low cost and simplest pack structure adopting by air cooling strategy, when batteries working as high-rate charge/discharge and the heat generation rate is larger, the strategy unable control the battery temperature in an expect range well [69]. This is due to the small heat capacity of cooling medium and low efficient of heat transfer. In this case, other cooling strategies may be more suitable, such as the liquid cooling strategy and PCM cooling strategy.

3.2 Liquid cooling

Compared to the air cooling strategy, a liquid type thermal management system could reduce more energy consumption and provide a better cooling effect [137].

For liquid cooling plate structure (Figure 4(a)), many cooling systems are designed as indirect cooling plate at the middle of two batteries [138]. Generally, simply physical structure of cooling plate is usually insufficient to achieve excellent thermal management goal. The physical dimension of the channel, such as its length, width, or route influences the effect of cooling plates, obviously. In order to

control the maximum temperature and the difference of local battery temperature, many optimization methods about liquid cooling plate channel quantity, mass flow rate, flow direction and entrance size were investigated in a study by Zhao [70]. Qian [139] compared different mini-channel cooling structure, cooling water flow rate, and direction of cooling water by simulation. Zhao [140] provide two considerable promises in improving the pack thermal uniformity, namely: (a) shortened the flow paths through increasing the flow channels, and (b) increasing the contact area between battery and the cooling channel. Due to the different heat generation rate distribution for large size battery, the flow direction has impact on the cooling effect. The literature [141] demonstrates that the cooling liquid unified inlet adjacent to the current collector tabs has merits as lower energy consumption, lower structure complexity, and higher cooling performance. Rao [141] experimented with mini-channel cooling plate. The result was that the pack's maximum temperature decreased, and the temperature deviation increased first and then decreased with flow rate of cooling liquid increasing. However, if the flow rate of cooling liquid increased continuously, the influence degree became weakened. The main thermal resistance of heat transfer existed in cooling ducts and there was thermal contact resistance with the battery [28]. In addition, increasing the flow rate of cooling liquid caused the energy consumption of pump increased dramatically. Ma [142] determined that with the mini-channel cooling flow rate increasing from 1L/min to 4L/min, the pump power increased near 47 times. Gao [143] embedded flexible graphite between the mini-channel and batteries to improve the uniformity of cooling performance. Wu [144] investigated Cu-water Nano-fluid as a battery thermal management cooling medium. The results indicated that nanoparticles can enhance heat transfer performance and reduce the uneven temperature distribution. Basu [51] offered a way to weld finned on the fluid side, the fin can used to fasten the battery and enlarge the heat exchange area.

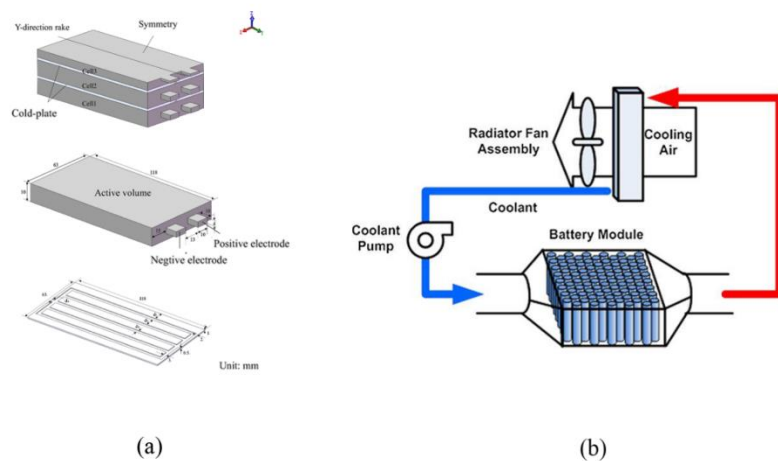


Figure 4. (a) Schematic of liquid cooling system: Module structure, Single battery and Cold-plate (“Reprinted from Energy Conversion and Management, 126, Z. Qian, Y. Li, Z. Rao, Thermal performance of lithium-ion battery thermal management system by using mini-channel cooling, 622-631, Copyright(2016), with permission from Elsevier.”); (b) configuration of direct liquid cooling BTMS (“Reprinted from Journal of Power Sources, 227, S. Park, D. Jung, Battery cell arrangement and heat transfer fluid effects on the parasitic power consumption and the cell temperature distribution in a hybrid electric vehicle, 191-198, Copyright(2013),with permission from Elsevier.”).

Liquid cooling plate have to bear thermal resistance of pipe structure, while batteries submerged in cooling liquid directly can give a bigger heat exchange area and lower thermal resistance [101]. Silicon oil as cooling media instead of air applied to the same pack structure can sharply increase system performance [145]. Regarding cylinder batteries, Park [137] presented a cooling structure similar with air cooling, and the cooling medium was mineral oil (electric insulation) (Figure 4(b)). Other liquid cooling media such as liquid metal (Gallium, etc.) can also provide a super cooling effect to the batteries than indirect cooling [73]. However, further study is necessary to solve problems of a direct cooling system, such as:

(1) The viscosity of cooling media. It should be heeded because it concerns energy consumption of BTMS and weight of packs;

(2) The stability of cooling media. It should exhibit excellent electrical insulation, flame retardant, and chemical stability. In addition, it should not corrode with batteries and packs;

(3) The sealing property of cooling system. The direct liquid cooling structure should be sealing well and benefit operational maintenance.

The optimum design of cooling plate structures for lowest average temperature is always different with the best temperature uniformity plates [146]. Therefore, when modifying the structures of cooling systems to meet the optimal cooling effect, it is worthy to consider the various sensitivity of parameters (temperature uniformity, average temperature or pressure drop) as a BTMS design guide [147]. In addition, a liquid cooling system exhibits excellent cooling effects, but it still is unable to prevent the occurrence of thermal runaway. The only way is to control the spread of thermal runaway [148].

3.3 Heat pipe cooling

The established technology of heat pipes can be divided into three sections: evaporator section, isothermal section, and condenser section [149]. The working process of heat pipe is that [150]: Firstly, liquid cooling medium absorbs heat and evaporates at evaporator section. Secondly, the liquid cooling medium moves from the isothermal section to condenser section, releases its heat, and changes into liquid. Finally, the liquid flows to evaporator section and continues to endothermic like the former. Due to the special heat conduction performance, lightweight and compact size, it also can be used to remove heat from the internal battery pack to outer [151-152].

The heat pipe transfer heat from evaporator section to the cooling media, and the heat must be absorbed from the cooling media to outer at condenser section to ensure it can work continuously. In turn, it is necessary to couple this with other methods to cool the condenser section of the heat pipe, such as forced air, thermostat, or water spray [153]. Wu [17] added aluminum fin to the heat pipe evaporating section, and condenser section which effectively improved the heat dissipation performance and met the BTMS requirement. Wang [154] and Rao [155] coupled heat pipe with PCM and outer air cooling strategies, which not only managed battery temperature well, but achieved PCM solidification to permit batteries to discharge and charge more cycles continuously before exceeding the restrictive temperature. Smith [156] applied the heat pipe to cooling the high power EV battery

pack, the condenser section of the heat pipe was cooling by liquid cooling plate. As compared to a conventional liquid cooling system, this coupled system provides less complicated design and leakage issues.

3.4 Phase change material cooling

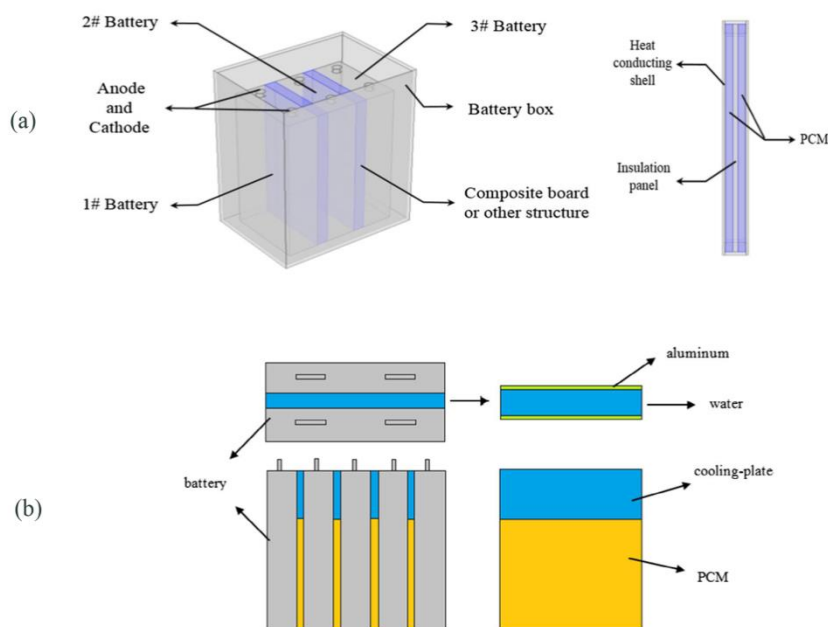


Figure 5. (a) Schematic of batteries module with PCM cooling plate (“Reprinted from Applied Thermal Engineering, 106, J. Yan, Q. Wang, K. Li, J. Sun, Numerical study on the thermal performance of a composite board in battery thermal management system, 131-140, Copyright(2016), with permission from Elsevier.”); (b) schematic of coupled cooling module with PCM/water cooling-plate (“Reprinted from Applied Thermal Engineering, 126, F. Bai, M. Chen, W. Song, Z. Feng, Y. Li, Y. Ding, Thermal management performances of PCM/water cooling-plate using for lithium-ion battery module based on non-uniform internal heat source, 17-27, Copyright(2017), with permission from Elsevier.”).

PCM has a more robust temperature controlling effect in battery thermal management. It could afford more uniform battery temperature distribution, and minimize the impact to surrounding batteries when thermal runaway occurred [157]. Yan [74] designed a sandwich structure of PCM board to cool the pack, and the result indicated that PCM board had excellent ability on the normal and abusing condition compared to general air or cooling board (Figure 5(a)).

Paraffin is always used in phase change materials, attributed to price and latent enthalpy. In consideration of low thermal conductivity [15], previous research proposed to meliorate paraffin composited with other materials, such as composite paraffin with nanoparticles [158], metal foam [159-161], Cu mesh [162], expanded graphite [53, 83], and carbon fiber [163]. Compound paraffin exhibits higher thermal conductivity and better temperature uniformity, oppositely lower latent enthalpy [164]. PCM with higher latent enthalpy can work at higher ambient temperature [165]. Also,

it could meet the particularly requirements for battery pack with the most appropriate thermal properties [166].

Other materials with appropriate phase transition temperatures also can be applied to battery thermal management such as pure octadecane [167]. Due to the time constant, the battery temperature was always higher than phase transition temperature when the phase change process occurred. Therefore, the rational utilization of phase change temperature and latent enthalpy of PCMs could keep batteries working at the appropriate temperature range [164].

To ensure the battery is working well under stressful conditions, the capacity of battery pack should be considered when the BTMS is designed to prevent thermal runaway [168]. Immersing battery into PCM and isolating them from each other could prevent the propagation of thermal runaway to adjacent ones [169-170]. A study by Al-Hallaj [171] showed that if the pack is working at 45°C ambient and 2C discharge rate, 90% capacity of the pack with PCM can be utilized while 50% without PCM before the battery temperature risen above safety limits.

Although PCM has an advantage for uniform temperature distribution, an obvious disadvantage of the PCM cooling system is that it fails to remove the heat of batteries which is far from the cooling medium [101]. Thus, adjusting batteries and PCM as closely as possible is necessary. Zhao [172-173] embedded PCM cores into cylindrical batteries, and it met the compact structure and high transfer efficiency. The experiment result has shown that such core BTMS consumes less PCM and achieves lower battery temperature rise and higher temperature uniformity than external BTMS. Meanwhile, Yan [74] pointed out that increasing the heat capacity of PCM could improve the heat dissipation effect of the pack. In addition, PCM worked as an energy storage medium; the thermal management system would fail if the heat did not diffuse from PCM to environment in a timely manner. For example, charging and discharging continually, the heat generated by batteries led to all PCM melting ultimately. Meanwhile, the temperature of PCM increased significantly because of running out of the latent enthalpy. Thus, it is necessary to combine PCM with other cooling strategies [174]. Ling [72] proposed that PCM be combined with forced-air cooling to improve cooling efficiency and reliability. Hémerly [157] coupled PCM with a liquid cooling system that could make liquid PCM solidified during a 2C charging period. Song [175] designed a semiconductor thermoelectric device/PCM coupled BTMS, through changing the arrangement of the semiconductor thermoelectric device and the temperature range of BTMS to optimizing the cooling /heating process. Generally, PCM directly cooling the batteries and be cooled by air/liquid which do not cooling batteries directly such as reference [176], these strategies can be summarized as series-coupled. In addition, the parallel-coupled was also researched: Xie [177] reported a pack structure that included two PCM tanks and air cooling structure. Both methods can cool batteries directly and cooperatively cool too. Due to the high cooling capacity of liquid cooling plate and the robust temperature uniform performance of PCM, parallel-coupled with PCM and liquid cooling plate: the liquid plate cooling the place where have a higher heat generation rate, and PCM cooling the other position. This strategy can both cooling the place where have the maximum temperature well and keep it have a higher temperature uniformity [178] (Figure 5(b)). Furthermore, in order to decrease non-uniform temperature of liquid cooling plate, Wang [179] used parallel-coupled force recycle air cooling strategy to keep temperature of packs uniformly. This strategy can increase heat transfer performance, lower the requirements of temperature difference

between batteries and inlet cooling water, as well as ensure the operation temperature and uniformity of batteries.

3.5 Other cooling strategies

Some novel battery thermal management strategies were studied in recent years. Mercedes Benz S400 [180] was first introduced refrigerant-based BTMS, which added a direct evaporator plate to the refrigerant circuit, and linked with the batteries. The most significant merit of the system is more compact and lightweight, but the obvious drawback is various components and complex control. Li [181] designed a battery cooling plate based on flow boiling in mini-channel, and drew a conclusion that a best Reynolds number could meet the peak of heat transfer performance, with the changing of the cooling medium flow rate. Al-Zareer [182-183] proposed to submerge batteries partly into liquid ammonia or liquid propane, and removed heat generated by batteries through a boiling heat transfer process. The limitation, however, was that these methods were only applied by HEV using ammonia and propane as fuels, respectively. van Gils [184] investigated boiling thermal management strategies based on pool boiling heat transfer principle. It adjusted the ambient pressure to keep heat transfer at nucleate boiling period which had a higher heat transfer coefficient, and to keep the cooling liquid a suitable boiling point at different conditions. Zhang [185] investigated that mini-channel was embedded into electrode layer, and put in electrolyte as cooling liquid. Based on the field synergy principle to analysis, the results showed that it could increase the cooling effect significantly than external cooling strategies. Ren [186] prepared a thin sodium alginate film with water content of 99%, stuck it to the wall of pack. In the system, water evaporated and absorbed heat when the temperature of pack increasing. The worn film which water was evaporated but it could recover when soaked it to water, then the film cooling method achieved lower cost and reutilization. Guo [187] demonstrated the feasibility of a 3D vapor chamber for BTMS, the vapor chamber is surrounding the battery and through the water vaporized in the chamber to cooling the battery.

Furthermore, previous researchers have put forward many coupled cooling strategies based on the different cooling characters of air, liquid, and PCM. And those methods exhibit different merits of cooling methods and prevent the defect of a single cooling method.

3.6 Battery heating strategies

Lithium-ion batteries exhibited poor performance in cold climates: the available capacity of batteries decreased, batteries resistance increased dramatically, charge/discharge became increased difficultly, and severe degradation led to poor cycle life. Battery heating equipment plays an important role to keep Li-ion battery working better at a lower temperature environment [188]. There are three types of battery heating methods: self-internal heating, convective heating, and mutual pulse heating [189] (Figure 6). Self-internal heating is obviously simple and efficient. It based on the batteries heat generation during charging/discharging to heating themselves. Ruan [190] put forward heating batteries through pulse charging and discharging, and adjusted the frequency and amplitude to improve

the heating performance. Zhang [191] inserted nickel foil into battery as heat generation device and connected with battery electrode when it needed to heating. The results revealed that the battery temperature could increase from -20°C to 0°C in 12.5 seconds and consumed little energy of battery. The convective heating strategy can heat the battery both internally and externally. The fan creates a convective flow and a resist heater converts electric power to heat the fluid. Song [192] added heating resistor into forced air BTMS, and heating batteries with convective. Lv [193] compared two kinds of battery heating strategies: forced air convection heating and silicone plate heating. The experiment result indicates that a “close-ended” structure pack is contribute to recycle the waste heat, and the silicone plate heating has batter performance in battery temperature uniformity and heating efficient. Mutual pulse heating strategy [189] was rarely studied by previous researchers. It utilizes battery output power to heating themselves. It divided the pack into two groups with equal capacity. The two groups charge for another group by turns, and switch at intervals of a period to balance the capacity of the two groups. The output power of the discharge group is used as the input power of the charge group. Since voltage required to charge batteries is higher than battery output voltage, a dc-dc converter is needed to boost battery’s discharge voltage.

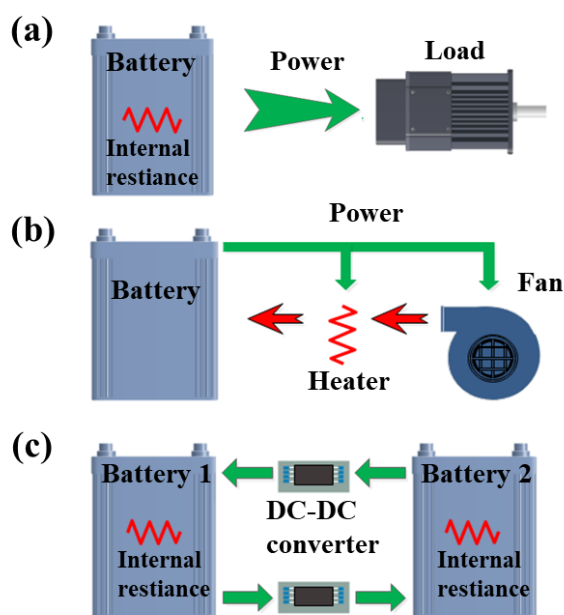


Figure 6. Heating strategies using battery power (a) self-internal heating, (b) convective heating, and (c) mutual pulse heating.

The energy consumption of battery heating system is mainly supplied by the pack itself, which also leads to the available capacity decrease and battery load increase. The expectant performances of battery heating strategy is short heating time, lower energy consumption and less damage to battery life [190]. Therefore, the ongoing study should mainly concern optimizing the battery heating process at different operating ambient temperature and decreasing the cost. The ultimate aim is to keep batteries working at an appropriate temperature.

4. CONTROL SYSTEM AND EVALUATION CRITERIA

The conventional battery management system (BMS) is used to measure the voltage and current of pack, predict electro-state, solve the uniformity state of batteries, and diagnose faults [194]. Similarly, BTMS is used to control the operation temperature of battery [195]. According to different working conditions, the control logic of BTMS also needs to optimize for improved cooling performance and reduced energy consumption.

4.1 Battery thermal management control systems

4.1.1. Macro-control measures

A conventional battery thermal management controlling system is designed with a temperature threshold. The cooling system starts to work when the battery temperature goes over the upper limit and halts when below the lower limit. Wang's experiment [196] indicated that the appropriate system could decrease energy consumption dramatically but increase the battery pack maximum temperature slightly.

In addition, applying the power of charging station for BTMS during charging at severe ambient to precooling or preheating could ensure batteries charged at a comfortable temperature and provide a comfortable battery temperature prepared for discharge. This strategy could save more battery energy during the journey, and avoid additional heat generation and increase output power [180].

4.1.2. Temperature difference adjustment

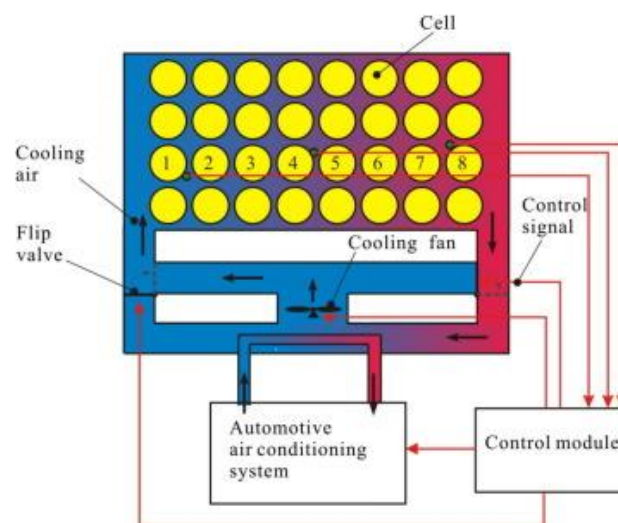


Figure 7. Schematic of reciprocate air cooling module, which the direction of cooling air is convertible (“Reprinted from International Journal of Heat and Mass Transfer, 83, F. He, L. Ma, Thermal management of batteries employing active temperature control and reciprocating cooling flow, 164-172, Copyright(2015), with permission from Elsevier.”).

During charging/discharging, battery temperatures will increase rapidly when the heat could not be dissipated to outer betimes. If the temperature of inlet cooling medium keeps constant or much lower than battery's temperature, the temperature difference between batteries and cooling medium will increase, and the temperature uniformity of batteries from inlet to outlet may worsen. As such, changing the temperature of cooling medium will keep a suitable temperature difference and a rational temperature rising between batteries, which may be a more sensible control strategy for a BTMS [143].

Due to the lower thermal capacity of cooling medium in air cooling system, the large temperature difference of air between inlet and outlet has always posed problems. Reciprocating air flow structure constantly adjusts the flow direction, and thus it reduces the variable of temperature difference between batteries and air in different positions. And adjusting reciprocating frequency of fan for variable air flow is adjusted can also improve the cooling effect [136] (Figure 7).

4.1.3. Outer cooling system

Two types of battery cooling systems can be defined as active cooling and passive cooling by whether assembling refrigeration equipment or not. The active features could make the temperature of system lower than ambient temperature with more power consumed, with passive cooling system just the opposite. The main role of outer cooling system is to remove heat from cooling medium generated by batteries. As for the passive cooling system, Nissan Leaf simply suction fresh air to cooling the battery pack, and the exhaust air emitted to ambient directly (Figure 8(a)). As for an active cooling system, Tesla utilized dual-circuit liquid cooling system, cooperating the air cooling system with refrigerant circuit to cooling the liquid medium (Figure 8(b)).

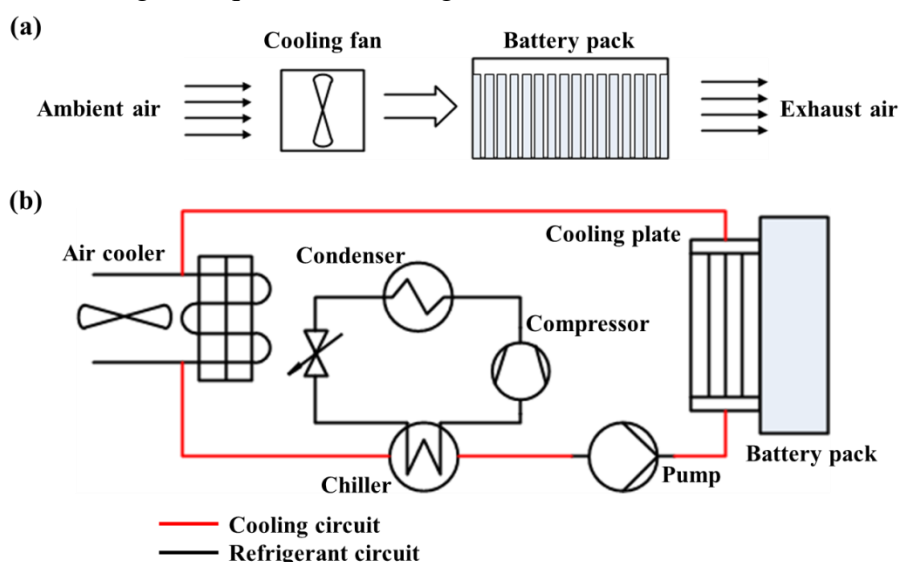


Figure 8. (a) Nissan Leaf battery cooling system and (b) Tesla's vehicle battery cooling system.

4.1.4. Safeguard procedures

For purpose of predicting thermal runaway, Shah [197] put forward a non-dimensional thermal parameter correlated with battery thermal conductivity, heat transfer coefficient and heat generation

rate. Based on the changing trends of this parameter to estimate battery states, and take relevant measures to cope with the battery thermal behavior. Reducing the operating SOC and charge/discharge rate of battery is an effective means to maintain the suitable working temperature range of the battery on the severe condition [121]. In addition, Altaf [198] devised a predictive control scheme for terminal voltage control and simultaneous thermal and SOC balancing of batteries. It used minimum future load information to lower the heat generation rate when the batteries temperature is high.

4.2 System evaluation criteria

There are rarely rigorous and universal standards used to evaluate the performance of specific BTMS before. Most previous research was merely concerned about the maximum temperature and maximum temperature difference of batteries. However, ambiguous comparisons may lead to incorrect directions toward optimization. Parameters reviewed below could be used as evaluating criteria, which merits further research in the future.

(1) The maximum temperature and maximum temperature difference of batteries. Generally speaking, the upper limit of temperature is 45°C during charging and 60°C during discharging. The temperature difference is 5°C. The location with maximum temperature may trigger thermal runaway. Uniform temperature distribution can ensure the aging speed of batteries homogeneously and prolong the cycle life of the pack.

(2) Variance and distribution function of battery temperature. The maximum temperature difference of batteries could not indicate the thermal uniformity level of pack. It is necessary to analyze temperature deviation statistically. Accordingly, uniform performance of different pack structures could be compared by variance and distribution function.

Other algorithm parameters may also be used to evaluate a pack's thermal uniformity. For instance, uniformity index T_{uni} [142] could be calculated by Eq. (10). T_{dif} is the biggest temperature differences of batteries, T_{avg} is the average temperature of batteries. Generally speaking, high ambient temperature always leads to a lower heat generation rate and temperature deviation, but it also damages the battery's life simultaneously. According to the definition, the smaller T_{uni} may meet the better cooling effect.

$$T_{uni} = \frac{T_{dif}}{T_{avg}}, \quad (10)$$

(3) Energy density or volume ratio of pack. The cooling system took up extra space and increased the mass and volume ratio of BTMS which may promote the cooling performance slightly [199], with the costs volume of pack increased and volume energy density decreased. For a PCM cooling system, the latent enthalpy and reliability of system could be increased with more PCM which may burden the battery power system. Contrasting different BTMSs with energy density or volume ratio of pack is very helpful for a pack design that targets lightweight and compact characteristics.

(4) Cooling effectiveness of BTMS [199]. It is defined as the ratio of practical heat exchanger capacity and theory maximum heat exchanger capacity. As seen Eq. (11), where T_l is location temperature of pack; T_{max} is the biggest temperature of pack. The use of cooling effectiveness can significantly indicate the cooling performance of designed strategies in different locations. In addition,

adjusting cooling effectiveness by inlet cooling medium temperature, and thus BTMS may work for high efficiency.

$$\eta_c = \frac{T_l - T_{avg}}{T_{max} - T_{avg}}, \quad (11)$$

(5) Energy consumption. As Section 3.2 described, for liquid cooling, increasing the flow rate of cooling water may improve the cooling effect and this change trends to weakness gradually. Meanwhile, the energy consumption of the pump increased dramatically. Moreover, high power required by BTMS also leads to high load and extra heat generation for batteries. As a result, the proper design of energy consumption also should be considered. Normally, energy consumption includes system resistance loss and outer cooling system load.

(6) Thermal runaway risk (TRR) score. The concept of TRR score was proposed by Wang [97, 200] and used to evaluate the safety of batteries with different materials under the same testing conditions. The robustness of BTMS designed for the pack according to the current quality and safety standards is also assessed by TRR score [188]. Generally, the TRR score can also describe the severity rating if battery thermal runaway occurred; the higher TRR score always means that the battery process had greater endurance in abusive conditions, lower energy released during explosion, or narrower spread range when thermal runaway occurred. The TRR score contributes to evaluate the security performance of the pack.

5. CONCLUSIONS AND OUTLOOK

BTMSs have drawn much interest for energy storage systems. Because of the considerable impacts of battery operating temperatures, two key functions of BTMSs are worth noting:

- (1) They provide a suitable operating temperature and thus ensure a high usage performance and long cycle life for packs;
- (2) They prevent thermal runaway from occurring and spreading and improve the safety.

The main contributions of this review are as follows:

(1) Lithium-ion battery characteristics related to their thermal performances were analyzed, two main parameters (thermal capacity and thermal conductivity) of batteries were introduced, and some problems related to the heat generation and dissipation in batteries were summarized. In addition, the thermal stabilities of battery materials and the possible hazards when thermal runaway occurs were also reviewed.

(2) The currently applied technologies for thermal management were introduced. Merits and demerits of various cooling strategies were analyzed, and many different optimization methods were compared. In addition, battery heating strategies applied in cold environments were mentioned.

(3) We reviewed four dimensions of BTMS control theory: macro-control measures, temperature difference adjustment, outer cooling systems, and safeguard procedures. Designing an appropriate control strategy for BTMSs plays a significant role for packs. Optimizing the system control strategy can reduce the required energy consumption and improve the performance of BTMSs.

(4) Some evaluation parameters from previous research were summarized, which can be used as BTMS evaluation criteria. This will help to optimize the design of BTMS from multiple points of view multi-views based on the different requirements of specific packs and finally acquire the most appropriate BTMS.

The thermal issues of lithium-ion batteries are important. For the design of BTMSs, the focus should be on the cooling or heating capacity, the system complexity, energy consumption, reliability, and maintenance costs. Batteries' heat generation rates are complicated and closely related to their states. This plays a dominant role in the BTMS design. More accurate models addressing battery heat generation may be researched. In addition, excellent control strategies of BTMSs can greatly improve their performances as well. Thus, more control strategies may be presented in the future. Furthermore, although various BTMSs have been designed in the past, their application was uneven. In addition, due to the characteristics of different BTMS strategies, ambiguous evaluation criteria cause difficulty in distinguishing good designs. Hence, establishment of a recognized and comprehensive evaluation system is eagerly awaited.

GLOSSARY

EV	electric vehicle	Q_{tot}	total heat generation rate
HEV	hybrid electric vehicle	Q_{irr}	irreversible heat generation rate
PHEV	plug-in hybrid electric vehicle	Q_{rev}	reversible heat generation rate
LCO	Li-Co lithium-ion battery	R_{int}	equivalent internal resistance
LFP	Li-Fe lithium-ion battery	I	working current
LMO	Li-Mn lithium-ion battery	T	battery temperature
NCM	Li-NiCoMn lithium-ion battery	E_{eq}	equilibrium electromotive force
SOH	state of health	C_p	heat capacity
BTMS	battery thermal management system	t	time
PCM	phase change material	T_{surf}	battery surface temperature
OCV	Open circuit voltage	T_{amb}	test ambient temperature
SOC	state of charge	R_{int}	thermal conductive resistance from the core of battery to surface
HTB	high temperature battery	R_{out}	heat convection resistance from the battery surface to ambient
RTB	room temperature battery	T_{in}	battery core temperature
CC	constant current	Φ	heat flux
GITT	galvanostatic intermittent titration technique	ΔT	thermal transfer temperature difference
EIS	electrochemical impedance spectroscopy	R	total thermal resistance
ARC	Accelerating Rate Calorimeter	h	convective heat transfer coefficient
SEI	solid electrolyte interphase	A	heat transfer area
CFD	computational fluid dynamics	T_{uni}	temperature uniformity index
BMS	battery management system	T_{dif}	The biggest temperature differences of batteries
TRR	thermal runaway risk	T_{avg}	average temperature of batteries
		T_l	location temperature of pack
		T_{max}	the biggest temperature of pack

ACKNOWLEDGMENTS

This work was supported by the Fund of Key Scientific and Technological Project of Henan Province (No.172102210349, 182102210079), the Science and Technology Planning Project of Guangdong Province, China (2015B010135006, 2017B010120002), and the Science and Technology Program of Guangzhou, China (201802010072).

References

1. H. Shareef, M. M. Islam and A. Mohamed, *Renew Sust Energ Rev*, 64 (2016) 403.
2. J. Vazquez-Arenas, L. E. Gimenez, M. Fowler, T. Han and S.-k. Chen, *Energy Convers Manage*, 87 (2014) 472.
3. H. Lundgren, P. Svens, H. Ekström, C. Tengstedt, J. Lindström, M. Behm and G. Lindbergh, *J Electrochem Soc*, 163 (2015) A309.
4. T. Yuksel, S. Litster, V. Viswanathan and J. J. Michalek, *J Power Sources*, 338 (2017) 49.
5. A. Friesen, F. Horsthemke, X. Mönnighoff, G. Brunklaus, R. Krafft, M. Börner, T. Risthaus, M. Winter and F. M. Schappacher, *J Power Sources*, 334 (2016) 1.
6. Q. Wang, P. Ping, X. Zhao, G. Chu, J. Sun and C. Chen, *J Power Sources*, 208 (2012) 210.
7. X. Feng, J. Sun, M. Ouyang, F. Wang, X. He, L. Lu and H. Peng, *J Power Sources*, 275 (2015) 261.
8. Z. Zhang, D. Fouchard and J. R. Rea, *J Power Sources*, 70 (1998) 16.
9. E. P. Roth, D. H. Doughty and J. Franklin, *J Power Sources*, 134 (2004) 222.
10. P. Peng and F. Jiang, *Int J Heat Mass Transfer*, 103 (2016) 1008.
11. J. S. Gnanaraj, E. Zinigrad, L. Asraf, H. E. Gottlieb, M. Sprecher, D. Aurbach and M. Schmidt, *J Power Sources*, 119-121 (2003) 794.
12. E. P. Roth, D. H. Doughty and D. L. Pile, *J Power Sources*, 174 (2007) 579.
13. C.-Y. Jhu, Y.-W. Wang, C.-Y. Wen and C.-M. Shu, *Appl Energ*, 100 (2012) 127.
14. P. Amiribavandpour, W. Shen, D. Mu and A. Kapoor, *J Power Sources*, 284 (2015) 328.
15. Z. Rao and S. Wang, *Renew Sust Energ Rev*, 15 (2011) 4554.
16. C. Yuan, Q. Wang, Y. Wang and Y. Zhao, *Appl Therm Eng*, 153 (2019) 39.
17. M. S. Wu, K. H. Liu, Y. Y. Wang and C. C. Wan, *J Power Sources*, 109 (2002) 160.
18. S. Panchal, I. Dincer, M. Agelin-Chaab, R. Fraser and M. Fowler, *Int Commun Heat Mass*, 71 (2016) 35.
19. S. A. Hallaj, H. Maleki, J. S. Hong and J. R. Selman, *J Power Sources*, 83 (1999) 1.
20. R. Arunachala, S. Arnold, L. Moraleja, T. Pixis, A. Jossen and J. Garche, *Influence of Cell Size on Performance of Lithium Ion Battery*, Battery Conference, Aachen, Germany, 2015,
21. L. H. Saw, Y. Ye and A. A. O. Tay, *Appl Energ*, 131 (2014) 97.
22. U. S. Kim, C. B. Shin and C.-S. Kim, *J Power Sources*, 180 (2008) 909.
23. Z. Yunyun, Z. Guoqing, W. Weixiong and L. Weixiong, *Heat Mass Transfer*, 50 (2014) 887.
24. G.-H. Kim, A. Pesaran and R. Spotnitz, *J Power Sources*, 170 (2007) 476.
25. N. Yang, X. Zhang, G. Li, A. Cai and Y. Xu, *Energy Technol-Ger*, 6 (2018) 1067.
26. Y. Chen and J. W. Evans, *J Electrochem Soc*, 140 (1993) 1833.
27. W. Tong, K. Somasundaram, E. Birgersson, A. S. Mujumdar and C. Yap, *Int J Therm Sci*, 94 (2015) 259.
28. A. Pesaran and G. H. Kim, *Battery Thermal Management System Design Modeling*, the 22nd International Battery, Hybrid and Fuel Cell Electric Vehicle Conference and Exhibition (EVS-22), Yokohama, Japan, 2006,
29. Q. Wang, B. Jiang, B. Li and Y. Yan, *Renew Sust Energ Rev*, 64 (2016) 106.
30. H. Liu, Z. Wei, W. He and J. Zhao, *Energy Convers Manage*, 150 (2017) 304.
31. J. F. Peters, M. Baumann, B. Zimmermann, J. Braun and M. Weil, *Renew Sust Energ Rev*, 67 (2017) 491.
32. C. Pastor-Fernández, K. Uddin, G. H. Chouchelamane, W. D. Widanage and J. Marco, *J Power*

- Sources, 360 (2017) 301.
33. M. Li, *Renew Energ*, 100 (2017) 44.
 34. S. Chacko and Y. M. Chung, *J Power Sources*, 213 (2012) 296.
 35. S. Panchal, I. Dincer, M. Agelin-Chaab, R. Fraser and M. Fowler, *Int J Therm Sci*, 99 (2016) 204.
 36. S. Panchal, I. Dincer, M. Agelin-Chaab, R. Fraser and M. Fowler, *Appl Therm Eng*, 96 (2016) 190.
 37. M. Mastali Majdabadi, S. Farhad, M. Farkhondeh, R. A. Fraser and M. Fowler, *J Power Sources*, 275 (2015) 633.
 38. S. Panchal, I. Dincer, M. Agelin-Chaab, R. Fraser and M. Fowler, *Appl Energ*, 180 (2016) 504.
 39. Y. Xing, W. He, M. Pecht and K. L. Tsui, *Appl Energ*, 113 (2014) 106.
 40. C. Edouard, M. Petit, C. Forgez, J. Bernard and R. Revel, *J Power Sources*, 325 (2016) 482.
 41. W. Situ, X. Yang, X. Li, G. Zhang, M. Rao, C. Wei and Z. Huang, *Int J Heat Mass Transfer*, 104 (2017) 743.
 42. J. Wu, Y. Wang, X. Zhang and Z. Chen, *J Power Sources*, 327 (2016) 457.
 43. K. Onda, T. Ohshima, M. Nakayama, K. Fukuda and T. Araki, *J Power Sources*, 158 (2006) 535.
 44. J.-K. Kim and C.-S. Lee, *Int J Pr Eng Man-GT*, 2 (2015) 255.
 45. N. Damay, C. Forgez, M.-P. Bichat and G. Friedrich, *J Power Sources*, 283 (2015) 37.
 46. S. Arora, W. Shen and A. Kapoor, *J Power Sources*, 350 (2017) 117.
 47. H. P. G. J. Beelen, L. H. J. Raijmakers, M. C. F. Donkers, P. H. L. Notten and H. J. Bergveld, *Appl Energ*, 175 (2016) 128.
 48. J. Gomez, R. Nelson, E. E. Kalu, M. H. Weatherspoon and J. P. Zheng, *J Power Sources*, 196 (2011) 4826.
 49. H. Kim, S. Kim, T. Kim, C. Hu and B. D. Youn, *Online thermal state estimation of high power lithium-ion battery*, 2015 IEEE Conference on Prognostics and Health Management (PHM), Austin, TX, USA, 2015, 1.
 50. M. Yildiz, H. Karakoc and I. Dincer, *Int Commun Heat Mass*, 75 (2016) 311.
 51. S. Basu, K. S. Hariharan, S. M. Kolake, T. Song, D. K. Sohn and T. Yeo, *Appl Energ*, 181 (2016) 1.
 52. D. Bernardi, E. Pawlikowski and J. Newman, *J Electrochem Soc*, 132 (1984) 5.
 53. A. Mills and S. Al-Hallaj, *J Power Sources*, 141 (2005) 307.
 54. A. Eddahech, O. Briat and J.-M. Vinassa, *Energy*, 61 (2013) 432.
 55. R. E. Williford, V. V. Viswanathan and J.-G. Zhang, *J Power Sources*, 189 (2009) 101.
 56. J. P. Schmidt, A. Weber and E. Ivers-Tiffée, *Electrochim Acta*, 137 (2014) 311.
 57. K. A. Murashko, A. V. Mityakov, V. Y. Mityakov, S. Z. Sapozhnikov, J. Jokiniemi and J. Pyrhönen, *J Power Sources*, 330 (2016) 61.
 58. Y. Inui, Y. Kobayashi, Y. Watanabe, Y. Watase and Y. Kitamura, *Energy Convers Manage*, 48 (2007) 2103.
 59. E. Schuster, C. Ziebert, A. Melcher, M. Rohde and H. J. Seifert, *J Power Sources*, 286 (2015) 580.
 60. J. Reyes-Marambio, F. Moser, F. Gana, B. Severino, W. R. Calderón-Muñoz, R. Palma-Behnke, P. A. Estevez, M. Orchard and M. Cortés, *J Power Sources*, 306 (2016) 636.
 61. X. M. Xu and R. He, *Renew Sust Energ Rev*, 29 (2014) 301.
 62. F. Richter, S. Kjelstrup, P. J. S. Vie and O. S. Burheim, *J Power Sources*, 359 (2017) 592.
 63. H. Maleki, H. Wang, W. Porter and J. Hallmark, *J Power Sources*, 263 (2014) 223.
 64. K. Jagannadham, *J Power Sources*, 327 (2016) 565.
 65. A. Loges, S. Herberger, P. Seegert and T. Wetzel, *J Power Sources*, 336 (2016) 341.
 66. A. Loges, S. Herberger, D. Werner and T. Wetzel, *J Power Sources*, 325 (2016) 104.
 67. D. Werner, A. Loges, D. J. Becker and T. Wetzel, *J Power Sources*, 364 (2017) 72.
 68. R. Liu, J. Chen, J. Xun, K. Jiao and Q. Du, *Appl Energ*, 132 (2014) 288.
 69. R. Sabbah, R. Kizilel, J. R. Selman and S. Al-Hallaj, *J Power Sources*, 182 (2008) 630.
 70. J. Zhao, Z. Rao and Y. Li, *Energy Convers Manage*, 103 (2015) 157.
 71. L. H. Saw, Y. Ye, A. A. O. Tay, W. T. Chong, S. H. Kuan and M. C. Yew, *Appl Energ*, 177 (2016)

783.

72. C. Lin, S. Xu, G. Chang and J. Liu, *J Power Sources*, 275 (2015) 742.
73. X.-H. Yang, S.-C. Tan and J. Liu, *Energy Convers Manage*, 117 (2016) 577.
74. J. Yan, Q. Wang, K. Li and J. Sun, *Appl Therm Eng*, 106 (2016) 131.
75. L. H. Saw, Y. Ye and A. A. O. Tay, *Energy Convers Manage*, 87 (2014) 367.
76. Z. Ling, F. Wang, X. Fang, X. Gao and Z. Zhang, *Appl Energ*, 148 (2015) 403.
77. J. Zhao, Z. Rao, Y. Huo, X. Liu and Y. Li, *Appl Therm Eng*, 85 (2015) 33.
78. S. Jung and D. Kang, *J Power Sources*, 248 (2014) 498.
79. R. Mahamud and C. Park, *J Power Sources*, 196 (2011) 5685.
80. L. Fan, J. M. Khodadadi and A. A. Pesaran, *J Power Sources*, 238 (2013) 301.
81. S. C. Chen, C. C. Wan and Y. Y. Wang, *J Power Sources*, 140 (2005) 111.
82. C. Forgez, D. Vinh Do, G. Friedrich, M. Morcrette and C. Delacourt, *J Power Sources*, 195 (2010) 2961.
83. K. K. Parsons, *J Therm Sci Eng Appl*, 9 (2017) 011012.
84. Y. Saito, K. Kanari, K. Takano and T. Masuda, *Thermochim Acta*, 296 (1997) 75.
85. J. Jiang and J. R. Dahn, *Electrochem Commun*, 6 (2004) 39.
86. Y. Wang, K. Zaghbi, A. Guerfi, F. F. C. Bazito, R. M. Torresi and J. R. Dahn, *Electrochim Acta*, 52 (2007) 6346.
87. W.-C. Chen, Y.-W. Wang and C.-M. Shu, *J Power Sources*, 318 (2016) 200.
88. K.-Y. Oh and B. I. Epureanu, *Appl Energ*, 178 (2016) 633.
89. J. Lamb and C. J. Orendorff, *J Power Sources*, 247 (2014) 189.
90. J. Zhu, T. Wierzbicki and W. Li, *J Power Sources*, 378 (2018) 153.
91. R. Spotnitz and J. Franklin, *J Power Sources*, 113 (2003) 81.
92. P. Röder, N. Baba and H. D. Wiemhöfer, *J Power Sources*, 248 (2014) 978.
93. G. Guo, B. Long, B. Cheng, S. Zhou, P. Xu and B. Cao, *J Power Sources*, 195 (2010) 2393.
94. S. Yayathi, W. Walker, D. Doughty and H. Ardebili, *J Power Sources*, 329 (2016) 197.
95. J. Sun, J. Li, T. Zhou, K. Yang, S. Wei, N. Tang, N. Dang, H. Li, X. Qiu and L. Chen, *Nano Energy*, 27 (2016) 313.
96. S. Dey, Z. A. Biron, S. Tatipamula, N. Das, S. Mohon, B. Ayalew and P. Pisu, *Control Eng Pract*, 56 (2016) 37.
97. H. Wang, E. Lara-Curzio, E. T. Rule and C. S. Winchester, *J Power Sources*, 342 (2017) 913.
98. E. P. Roth and D. H. Doughty, *J Power Sources*, 128 (2004) 308.
99. B. K. Mandal, A. K. Padhi, Z. Shi, S. Chakraborty and R. Filler, *J Power Sources*, 161 (2006) 1341.
100. R. M. Spotnitz, J. Weaver, G. Yeduvaka, D. H. Doughty and E. P. Roth, *J Power Sources*, 163 (2007) 1080.
101. G. Karimi and X. Li, *Int J Energ Res*, 37 (2013) 13.
102. U. S. Kim, J. Yi, C. B. Shin, T. Han and S. Park, *J Power Sources*, 196 (2011) 5115.
103. H. He, R. Xiong and J. Fan, *Energies*, 4 (2011) 582.
104. S. Panchal, I. Dincer, M. Agelin-Chaab, M. Fowler and R. Fraser, *Int Commun Heat Mass*, 81 (2017) 210.
105. J. Jiang, H. Ruan, B. Sun, W. Zhang, W. Gao, L. Y. Wang and L. Zhang, *Appl Energ*, 177 (2016) 804.
106. C. Zhang, K. Li, J. Deng and S. Song, *IEEE T Ind Electron*, 64 (2017) 654.
107. M. Farag, H. Sweity, M. Fleckenstein and S. Habibi, *J Power Sources*, 360 (2017) 618.
108. M. Guo, G.-H. Kim and R. E. White, *J Power Sources*, 240 (2013) 80.
109. C. D. Rahn and C. Y. Wang, *Battery Systems Engineering*. John Wiley & Sons, Ltd, (2013)
110. C. Lin, C. Cui and X. Xu, *Lithium-ion battery electro-thermal model and its application in the numerical simulation of short circuit experiment*, the 27th International Battery, Hybrid and Fuel Cell Electric Vehicle Conference and Exhibition (EVS-27), Barcelona, Spain, 2013, 1.

111. Z. Li, J. Zhang, B. Wu, J. Huang, Z. Nie, Y. Sun, F. An and N. Wu, *J Power Sources*, 241 (2013) 536.
112. J. Zhu, Z. Sun, X. Wei and H. Dai, *Energies*, 10 (2017) 60.
113. C. Zhang, K. Li and J. Deng, *J Power Sources*, 302 (2016) 146.
114. M. Wang and H.-X. Li, *IEEE T Ind Electron*, 64 (2017) 2316.
115. R. R. Richardson, P. T. Ireland and D. A. Howey, *J Power Sources*, 265 (2014) 254.
116. R. R. Richardson, S. Zhao and D. A. Howey, *J Power Sources*, 326 (2016) 377.
117. R. R. Richardson, S. Zhao and D. A. Howey, *J Power Sources*, 327 (2016) 726.
118. H. Park, *J Power Sources*, 239 (2013) 30.
119. Z. Lu, X. Z. Meng, L. C. Wei, W. Y. Hu, L. Y. Zhang and L. W. Jin, *Energ Procedia*, 88 (2016) 682.
120. A. A. Pesaran, *J Power Sources*, 110 (2002) 377.
121. X. M. Xu and R. He, *J Power Sources*, 240 (2013) 33.
122. Z. Liu, Y. Wang, J. Zhang and Z. Liu, *Appl Therm Eng*, 66 (2014) 445.
123. X. Li, F. He, G. Zhang, Q. Huang and D. Zhou, *Appl Therm Eng*, 146 (2019) 866.
124. X. Li, F. He and L. Ma, *J Power Sources*, 238 (2013) 395.
125. T. Wang, K. J. Tseng, J. Zhao and Z. Wei, *Appl Energ*, 134 (2014) 229.
126. S. K. Mohammadian and Y. Zhang, *J Power Sources*, 273 (2015) 431.
127. F. He, X. Li and L. Ma, *Int J Heat Mass Transfer*, 72 (2014) 622.
128. J. Xie, Y. Xie and C. Yuan, *Int J Heat Mass Transfer*, 129 (2019) 1184.
129. K. Chen, S. Wang, M. Song and L. Chen, *Appl Therm Eng*, 123 (2017) 177.
130. H. He, H. Jia, W. Huo and F. Sun, *Energies*, 10 (2017) 81.
131. J. Xun, R. Liu and K. Jiao, *J Power Sources*, 233 (2013) 47.
132. T. Yang, N. Yang, X. Zhang and G. Li, *Int J Therm Sci*, 108 (2016) 132.
133. K. Chen, S. Wang, M. Song and L. Chen, *Int J Heat Mass Transfer*, 111 (2017) 943.
134. Z. Lu, X. Yu, L. Wei, Y. Qiu, L. Zhang, X. Meng and L. Jin, *Appl Therm Eng*, 136 (2018) 28.
135. X. Zhang, W. Wang, H. He, L. Hua and J. Heng, *Appl Therm Eng*, 112 (2017) 1297.
136. F. He and L. Ma, *Int J Heat Mass Transfer*, 83 (2015) 164.
137. S. Park and D. Jung, *J Power Sources*, 227 (2013) 191.
138. H. Yuan, L. Wang and L. Wang, *J Automotive Safety & Energy*, (2012)
139. Z. Qian, Y. Li and Z. Rao, *Energy Convers Manage*, 126 (2016) 622.
140. C. Zhao, A. C. M. Sousa and F. Jiang, *Int J Heat Mass Transfer*, 129 (2019) 660.
141. Y. Huo, Z. Rao, X. Liu and J. Zhao, *Energy Convers Manage*, 89 (2015) 387.
142. C. Journal of Thermal Science and Engineering Applications Lan, J. Xu, Y. Qiao and Y. Ma, *Appl Therm Eng*, 101 (2016) 284.
143. T. Zhang, Q. Gao, G. Wang, Y. Gu, Y. Wang, W. Bao and D. Zhang, *Appl Therm Eng*, 116 (2017) 655.
144. F. Wu and Z. Rao, *Appl Therm Eng*, 115 (2017) 659.
145. G. Karimi and A. R. Dehghan, *IJMEM*, 1 (2012) 88.
146. A. Jarrett and I. Y. Kim, *J Power Sources*, 196 (2011) 10359.
147. A. Jarrett and I. Y. Kim, *J Power Sources*, 245 (2014) 644.
148. J. Xu, C. Lan, Y. Qiao and Y. Ma, *Appl Therm Eng*, 110 (2017) 883.
149. B. Zohuri, *Heat pipe design and technology: Modern applications for practical thermal management, second edition*. Springer, Cham, (2016) Germany.
150. D. A. Reay, P. A. Kew and R. J. Mcglen, *Ph Tec*, 3 (2013) 311.
151. D. Worwood, Q. Kellner, M. Wojtala, W. D. Widanage, R. McGlen, D. Greenwood and J. Marco, *J Power Sources*, 346 (2017) 151.
152. N. Putra, B. Ariantara and R. A. Pamungkas, *Appl Therm Eng*, 99 (2016) 784.
153. R. Zhao, J. Gu and J. Liu, *J Power Sources*, 273 (2015) 1089.
154. W. Wu, X. Yang, G. Zhang, K. Chen and S. Wang, *Energy Convers Manage*, 138 (2017) 486.

155. J. Zhao, P. Lv and Z. Rao, *Exp Therm Fluid Sci*, 82 (2017) 182.
156. J. Smith, R. Singh, M. Hinterberger and M. Mochizuki, *Int J Therm Sci*, 134 (2018) 517.
157. C.-V. Hémerly, F. Pra, J.-F. Robin and P. Marty, *J Power Sources*, 270 (2014) 349.
158. G. Karimi, M. Azizi and A. Babapoor, *J Energy Storage*, 8 (2016) 168.
159. N. Javani, I. Dincer, G. F. Naterer and G. L. Rohrauer, *Appl Therm Eng*, 73 (2014) 307.
160. W. Q. Li, Z. G. Qu, Y. L. He and Y. B. Tao, *J Power Sources*, 255 (2014) 9.
161. Z. G. Qu, W. Q. Li and W. Q. Tao, *Int J Hydrogen Energy*, 39 (2014) 3904.
162. Y. Lv, X. Yang, X. Li, G. Zhang, Z. Wang and C. Yang, *Appl Energ*, 178 (2016) 376.
163. F. Samimi, A. Babapoor, M. Azizi and G. Karimi, *Energy*, 96 (2016) 355.
164. Z. Rao, S. Wang and G. Zhang, *Energy Convers Manage*, 52 (2011) 3408.
165. Y. Huo and Z. Rao, *Energy Convers Manage*, 133 (2017) 204.
166. Z. Ling, J. Chen, X. Fang, Z. Zhang, T. Xu, X. Gao and S. Wang, *Appl Energ*, 121 (2014) 104.
167. M. Alipanah and X. Li, *Int J Heat Mass Transfer*, 102 (2016) 1159.
168. P. T. Coman, E. C. Darcy, C. T. Veje and R. E. White, *Appl Energ*, 203 (2017) 189.
169. R. Kizilel, R. Sabbah, J. R. Selman and S. Al-Hallaj, *J Power Sources*, 194 (2009) 1105.
170. S. Wilke, B. Schweitzer, S. Khateeb and S. Al-Hallaj, *J Power Sources*, 340 (2017) 51.
171. R. Kizilel, A. Lateef, R. Sabbah, M. M. Farid, J. R. Selman and S. Al-Hallaj, *J Power Sources*, 183 (2008) 370.
172. R. Zhao, J. Gu and J. Liu, *Int J Energ Res*, 42 (2018) 2728.
173. R. Zhao, J. Gu and J. Liu, *Energy*, 135 (2017) 811.
174. S. A. Khateeb, M. M. Farid, J. R. Selman and S. Al-Hallaj, *J Power Sources*, 128 (2004) 292.
175. W. Song, F. Bai, M. Chen, S. Lin, Z. Feng and Y. Li, *Appl Therm Eng*, 137 (2018) 203.
176. H. Fathabadi, *Energy*, 70 (2014) 529.
177. S. Shi, Y. Xie, M. Li, Y. Yuan, J. Yu, H. Wu, B. Liu and N. Liu, *Energy Convers Manage*, 138 (2017) 84.
178. F. Bai, M. Chen, W. Song, Z. Feng, Y. Li and Y. Ding, *Appl Therm Eng*, 126 (2017) 17.
179. S. Wang, Y. Li, Y.-Z. Li, Y. Mao, Y. Zhang, W. Guo and M. Zhong, *Appl Therm Eng*, 123 (2017) 929.
180. B. Scrosati, J. Garche and W. Tillmetz, *Advances in Battery Technologies for Electric Vehicles*. Woodhead Publishing, (2015) Cambridge, UK.
181. Z. An, L. Jia, X. Li and Y. Ding, *Appl Therm Eng*, 117 (2017) 534.
182. M. Al-Zareer, I. Dincer and M. A. Rosen, *Electrochim Acta*, 247 (2017) 171.
183. M. Al-Zareer, I. Dincer and M. A. Rosen, *J Power Sources*, 363 (2017) 291.
184. R. W. van Gils, D. Danilov, P. H. L. Notten, M. F. M. Speetjens and H. Nijmeijer, *Energy Convers Manage*, 79 (2014) 9.
185. S. K. Mohammadian, Y.-L. He and Y. Zhang, *J Power Sources*, 293 (2015) 458.
186. Y. Ren, Z. Yu and G. Song, *J Power Sources*, 360 (2017) 166.
187. J. Gou and W. Liu, *Appl Therm Eng*, 152 (2019) 362.
188. M. Khan, M. Swierczynski and S. Kær, *Batteries*, 3 (2017) 9.
189. Y. Ji and C. Y. Wang, *Electrochim Acta*, 107 (2013) 664.
190. H. Ruan, J. Jiang, B. Sun, W. Zhang, W. Gao, L. Y. Wang and Z. Ma, *Appl Energ*, 177 (2016) 771.
191. G. Zhang, S. Ge, T. Xu, X.-G. Yang, H. Tian and C.-Y. Wang, *Electrochim Acta*, 218 (2016) 149.
192. Z. Song, H. Hofmann, J. Li, J. Hou, X. Zhang and M. Ouyang, *Appl Energ*, 159 (2015) 576.
193. Y. Lv, X. Yang, G. Zhang and X. Li, *Int J Heat Mass Transfer*, 128 (2019) 392.
194. L. Lu, X. Han, J. Li, J. Hua and M. Ouyang, *J Power Sources*, 226 (2013) 272.
195. S. Jung, S. H. Park and B. C. Choi, *Int J Auto Tech-Kor*, 18 (2017) 117.
196. H. Wang, W. Xu and L. Ma, *Int J Heat Mass Transfer*, 102 (2016) 315.
197. K. Shah, D. Chalise and A. Jain, *J Power Sources*, 330 (2016) 167.
198. F. Altaf, E. Bo and L. J. Mårdh, *IEEE T Contr Syst T*, 25 (2016) 47.
199. N. Javani, I. Dincer, G. F. Naterer and B. S. Yilbas, *Int J Heat Mass Transfer*, 72 (2014) 690.

200. F. Ren, T. Cox and H. Wang, *J Power Sources*, 249 (2014) 156.

© 2019 The Authors. Published by ESG (www.electrochemsci.org). This article is an open access article distributed under the terms and conditions of the Creative Commons Attribution license (<http://creativecommons.org/licenses/by/4.0/>).